Environmental Aspects of Operating Various Gas Microturbines

Abdolreza Zaltash, Andrei Petrov & D. Tom Rizy
Oak Ridge National Laboratory (ORNL)
Cooling, Heating and Power (CHP) Group
Engineering Science and Technology Division
Oak Ridge, Tennessee

Rick Langley & Eric Hubbard
EPRI PEAC
Knoxville, Tennessee

ABSTRACT

The variety of new distributed generation (DG) technologies, such as gas microturbine generators (MTGs), as well as Integrated Energy Systems (IES) has increased markedly over the last several years. Environmental issues are among one of the most important aspects of operating these systems. The subject of this paper is the emissions of various makes and sizes of MTGs. For the DG emissions tests, several MTGs of the size range of 30 to 80 kW were operated at outside ambient conditions. The two basic emissions components – carbon monoxide (CO) and nitrogen oxides (NO_x) – were given particularly close attention. For each MTG, emissions at steady-state operation were measured at different power output levels. For transient tests the emissions were measured as the MTG power output varied during startup, shutdown and from one setting to another for power dispatching. Evaluation of the various emission levels for the different MTGs was performed. Compliance of these emissions with existing environmental regulations (U.S. and California) and manufacturer's data is discussed.

INTRODUCTION

The conversion of electric energy production in the U.S. and other developed countries from a vertically integrated and regulated business to deregulation has created an important opportunity for distributed energy technologies [1, 2]. In the 2001 report by the National Energy Policy Development Group, the concept of Combined Cooling, Heating and Power (CHP), now currently known as Integrated Energy Systems (IES), is identified as a strategy for addressing increased energy demands and peak power issues [3]. Recent developments in distributed generation (DG) technologies have made available new opportunities for relatively small-scale IES that can be used in commercial buildings. DG in combination with thermally-activated technologies (TAT), which use waste heat directly for heating purposes or thermally-driven desiccant dehumidification or absorption cooling, provide important opportunities for IES to be a viable technology for buildings [1, 4].

Natural gas-fired combustion turbine generators, reciprocating engine generators, and microturbine generators (MTGs), technologies are achieving an increasingly important position in the IES market. At the same time the world standards for emissions are becoming increasingly more stringent [5]. In addition to the U.S. Environmental Protection Agency (EPA), many U.S. states (including California and New York) are attempting to set their own emission limits for the operation of DG equipment. For example, new 2003 Air District Guidelines for DG emissions issued in California stipulate that for an MTG with less than 3 MW power output, the nitrogen oxides (NO_x) and carbon monoxide (CO) emissions should not exceed 0.5 and 0.4 lb/MWh, respectively. Current 2003 standards adopted by the California Air Resources Board (CARB) are slightly less stringent ─ the NO_x and CO limits in DG exhaust gas are set at 0.5 and 6.0 lb/MWh, respectively, but by the year 2007 these limits will become dramatically more

restrictive at 0.07 and 0.10 lb/MWh, respectively [6]. Thus, the motivation to evaluate existing MTGs currently in use for DG and IES power production in order to see how well they comply with existing limits and what changes may be required in order to meet future emissions limits.

TEST EQUIPMENT

The four MTGs evaluated in this emissions study include:

- A 30-kW MTG ("MTG A") installed at the IES Test Laboratory, Oak Ridge National Laboratory (ORNL). Its detailed description is given in [7].
- A 30-kW MTG ("MTG B") installed at the EPRI PEAC. It is similar to "MTG A" but includes both grid-connect and grid-independent modes of operation. "MTG A" only allows grid-connect operation
- A 70-kW MTG ("MTG C") installed at EPRI PEAC. This MTG has a built-in air-to-water heat recovery unit (HRU) for recovering waste heat from the exhaust gas.
- An 80-kW MTG ("MTG D") installed at EPRI PEAC.

EMISSIONS MONITORING

The EPA lists six criteria air pollutants for which ambient air limits have been set [8-10]. These air pollutants include nitrogen oxide (NO_x), carbon monoxide (CO), sulfur dioxide (SO_2), lead (Pb), ozone (O_3) and particulates. NO_x, CO, and SO_2 are the most relevant of these pollutants, for the operation of natural gas-fired MTG-based IES systems. The most significant of the nitrogen oxides (NO_x) that are produced in high temperature combustion is nitric oxide (NO), which subsequently oxidizes in the atmosphere to produce nitrogen dioxide (NO_2). CO is a poisonous gas formed when carbon based fuels are not fully burned. SO_2 is formed at high combustion temperatures [9]. As gas temperature decreases, a portion of SO_2 is converted into SO_3, which reacts with water vapor contained in the flue gas to form sulfuric acid. The formation of this acid can result in the corrosion of low-temperature sections of the IES system. All these gases can have a significant effect on the level of environmental pollution and were given the most attention during this project's MTG emissions studies.

NO_x formation is minimized at lower combustion temperatures, but lower combustion temperatures also result in higher CO emissions [10, 11]. Thus, in order to achieve lower emissions levels, the MTG needs to be operated at a high air to fuel ratio (excess air) within the primary combustion zone of the unit. The excess air and carbon dioxide (CO_2, a "Green House" gas) emissions were calculated with a flue gas analyzer from the fuel data and oxygen concentration. The latter was measured with an oxygen electrochemical cell. The SO_2 concentration was also determined by the electrochemical cell method. The accuracy of the emissions measurements was within ±2% of these readings [12].

Excess air, CO_2, and O_2 concentrations were expressed in %, while NO_x, CO, and SO_2 concentrations were measured in ppm by volume (ppmV, *i.e.* volume of gaseous pollutant per million volumes of ambient air) at the test O_2 concentration. The latter were corrected to a common basis of 15% O_2 (standard used to compare different units) and converted to units used in ambient air monitoring, namely, mg/m^3 and lb/MWh.

The following Equations (1) to (3) were used to correct the concentrations in ppmV at the test O_2 concentration to ppmV at 15% O_2 concentration:

$$NO_{x\_15\%} = (NO_x - NO_{x\_a}) \cdot \left(\frac{5.9}{20.9 - O_2} \right) \cdot n \quad (1),$$

where: $NO_{x\_15\%}$ is the NO_x concentration at 15% O_2, ppmV; NO_x is the NO_x concentration measured during the tests, ppmV; NO_{x_a} is the ambient NO_x concentration, ppmV; O_2 is the O_2 concentration measured during the tests, %; and n is the ambient correction factor (available from [13]).

$$CO_{15\%} = (CO - CO_a - 0.088 \cdot THC_a) \cdot \left(\frac{5.9}{20.9 - O_2} \right) \quad (2),$$

where: $CO_{15\%}$ is the CO concentration at 15% O_2, ppmV; CO is the CO concentration measured during the tests, ppmV; CO_a is the ambient CO concentration, ppmV; THC_a is the ambient total hydrocarbon concentration, ppmV; and O_2 is the O_2 measured during the tests, %.

$$SO_{2\_15\%} = (SO_2 - SO_{2\_a}) \cdot \left(\frac{5.9}{20.9 - O_2} \right) \quad (3),$$

where: $SO_{2\_15\%}$ is the SO_2 concentration at 15% O_2, ppmV; SO_2 is the SO_2 concentration measured during the tests, ppmV; SO_{2_a} is the ambient SO_2, ppmV; and O_2 is the O_2 concentration measured during the tests, %.

Assuming that the ambient levels of CO, NO_x, SO_2, and total hydrocarbons are equal to or very close to zero, and that the ambient correction factor is close to unity, Equations (1)-(3) may be written as:

$$NO_{x\_15\%} = \frac{5.9 \cdot NO_x}{(20.9 - O_2)} \quad (4),$$

$$CO_{15\%} = \frac{5.9 \cdot CO}{(20.9 - O_2)} \quad (5),$$

$$SO_{2\_15\%} = \frac{5.9 \cdot SO_2}{(20.9 - O_2)} \quad (6).$$

These corrected values were then converted to mg/m^3 with the following equation [14]:

$$C_{mg/m^3} = \frac{12.187 \cdot C_{ppmV_{15}} \cdot M}{(273.15 + t)} \quad (7),$$

where: C_{mg/m^3} is the concentration of gaseous pollutant, mg/m^3; $C_{ppmV_{15}}$ is the concentration of gaseous pollutant, ppmV at 15% O_2 [from Equations (4)-(6)]; M is the molecular weight of the gaseous pollutant, g/mole; and t is the temperature of conversion (in this case 25°C).

Finally, the concentration of pollutant in lb/MWh was determined with the following equation:

$$C_{lbs/MWh} = C_{ppm} \cdot K_{\rho} \cdot F_d \cdot Q \cdot (\frac{20.9}{20.9 - O_2}) \quad (8),$$

where: $C_{lbs/MWh}$ is the concentration of gaseous pollutant, lb/MWh; C_{ppm} is the concentration of gaseous pollutant measured during the tests, ppm; K_{ρ} is the gas density conversion, lb/(SCF·ppm); F_d is the ratio of the dry gas volume of the products of combustion to the heat content of the fuel (dry F-factor) specified in [15], SCF/MMBtu (MMBtu is a unit of one million Btus or 10 therms); O_2 is the O_2 concentration measured during the tests, %; and Q is the heat rate, MMBtu/MWh. The latter is calculated as follows:

$$Q = (\frac{100}{E_f \cdot \eta}) \quad (9),$$

where: E_f = 0.29283 is the energy conversion factor, MWh/MMBtu; η is the process efficiency, %.

RESULTS

The emissions studies of MTGs A, B, and D were performed over a wide range of electric power output. Since MTG C is designed to only operate at one setting which cannot be changed, the emissions tests were performed at 60 kW power output since this is what the MTG was capable of producing for the ambient conditions on the day of the tests. The ambient temperature during most of the tests was within the range of 18 to 21°C (65-70°F). For the steady-state tests, MTG emissions were measured at different power output levels for 15 to 20 minute periods. For transient tests, emissions levels were measured as the MTG power output was varied during startup, shutdown, and power dispatch (increase or decrease of power output).

Effect of Power Output on Emissions Rate of Two Similar 30-kW MTGs A and B

The tests were performed over the MTG power output ranges of 1/10 (3 kW) to full power output (28 kW) for MTG A and 0 to full power output (28 kW) for MTG B[1]. Figures 1-6 present the dependencies of NO_x, and CO emissions on power output level in ppmV at 15% O_2 ($ppmV_{15}$), mg/m^3, and lb/MWh. Although there are some differences in absolute emissions values for these two MTGs, the general trends are the same and similar to those reported previously [7].

The minimum rate of emissions is observed at full power output (28 kW): 0-19 $ppmV_{15}$ (0-22 mg/m^3 or 0-0.7 lb/MWh) CO and *ca.* 6 $ppmV_{15}$ (11 mg/m^3 or 0.4 lb/MWh) NO_x. These data are within the limits specified by the MTG manufacturer which is 40 $ppmV_{15}$ CO (1.32 lb/MWh) and 9 $ppmV_{15}$ (0.49 lb/MWh) NO_x. The NO_x concentration in the MTG flue gas at full power is significantly lower than the data reported for a 100 kW reciprocating engine (100 $ppmV_{15}$ or 47 lb/MWh NO_x) [16].

[1] The ambient temperature during both tests for the output up to 25 kW was 18 to 21°C (65-70°F); emissions results for 28 kW output are given for the ambient temperature 7 to10°C (45-50°F).

The measured full-load emissions of MTGs A and B are within the limits recently introduced by CARB for DG equipment and are on the threshold of the Air District Guidelines. It should be noted that the emissions expressed in lb/MWh are related to the electrical power conversion (maximum efficiency around 23%), but if we consider the IES operation of the MTG in combination with thermally-activated equipment, whereby the efficiency can reach 60%, then the CO and NO_x levels in flue gas would be reduced to 0-0.3 and 0.1 lb/MWh, respectively. These MTG based IES emissions levels would be well within both the CARB and air district emissions limits.

However, it should be noted that decreasing the MTG power output significantly changes the emission rate of the above-mentioned contaminants. In addition, there is a large variation in the emissions at the 20 kW output depending on whether the power output is being ramped up or down. For example, the CO level at 20 kW after the output decreases from 25 kW is about 159-223 $ppmV_{15}$, and after the output increases from 15 kW is about 11 $ppmV_{15}$. On the other hand, the NO_x emissions trend is the inverse of the CO trend: *ca.* 3 and 73-80 $ppmV_{15}$, respectively. Thus, depending on the direction of power dispatch to arrive at the operating point of 20 kW, it is possible to have either high CO and low NO_x emission levels (decreasing from 25 kW) or vice versa (increasing from 15 kW). The nature of this phenomenon is unknown, however, it is likely due to the specific controller/control schemes of these units. This phenomenon was not observed at other MTG power output settings.

The emissions results clearly indicate that operating at power outputs below 25 kW will result in exceeding the emission limits specified by the manufacturer of MTGs A and B. This especially occurs at high ambient temperatures when the turbine speed reaches its maximum allowable limit causing a decrease in turbine power output.

The major difference from the previous tests [6] is the lack of SO_2 in emission samples. SO_2 was detected only during turbine startup with a maximum amount of *ca*. 14 $ppmV_{15}$ (Figure 7). This may be the result of improved quality of pipeline gas.

Figure 7 shows the dynamic change in emissions with time and power output. Note the high CO peak during startup, the existence of NO_2 oxide in addition to NO below 20 kW, as well as the CO and NO_x behavior at 20 kW output and the lack of SO_2 discussed above.

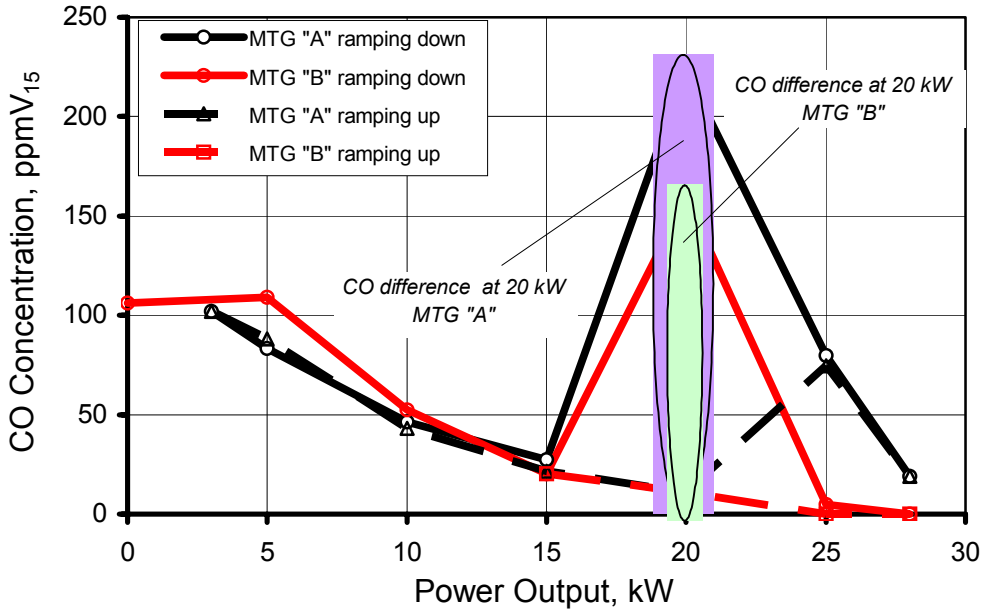

Figure 1. CO Concentration ($ppmV_{15}$) Versus the Power Output of MTGs A and B.

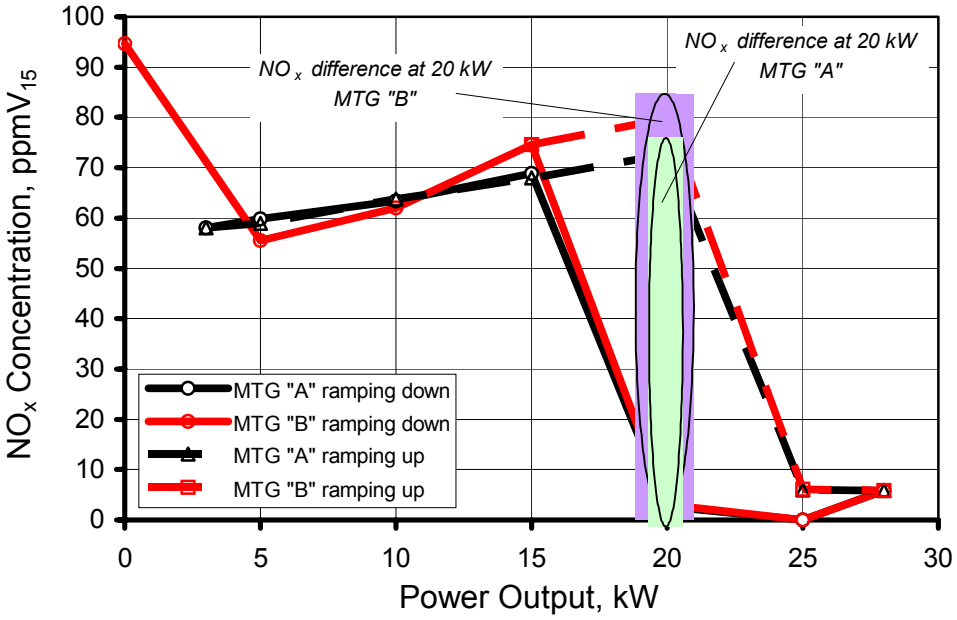

Figure 2. NO_x Concentration ($ppmV_{15}$) Versus the Power Output of MTGs A and B.

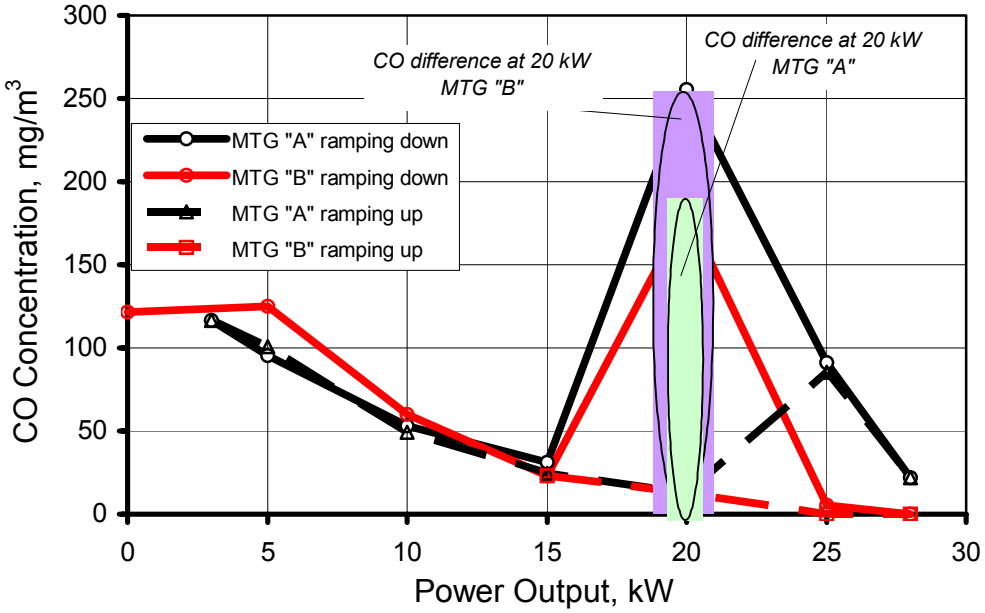

Figure 3. CO Concentration (mg/m^3) Versus the Power Output of MTGs A and B.

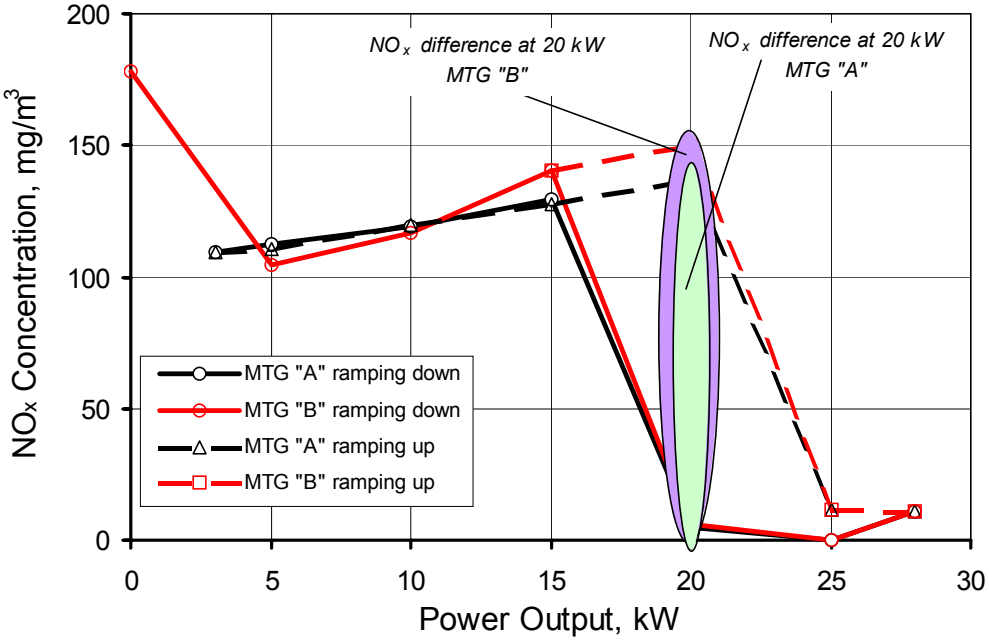

Figure 4. NO_xConcentration (mg/m^3) Versus the Power Output of MTGs A and B.

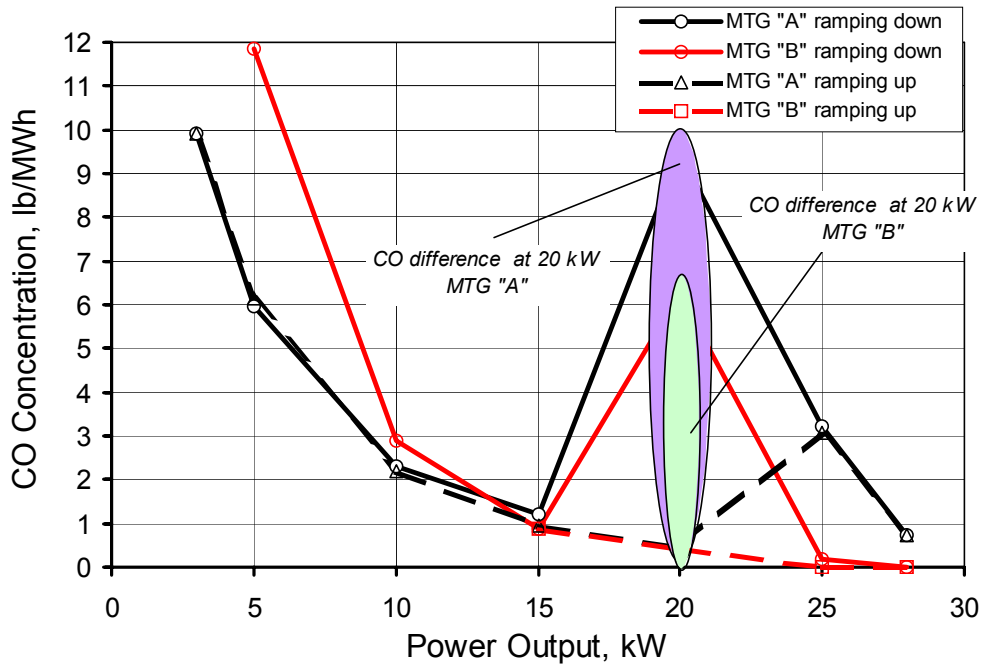

Figure 5. CO Concentration (lb/MWh) Versus the Power Output of MTGs A and B.

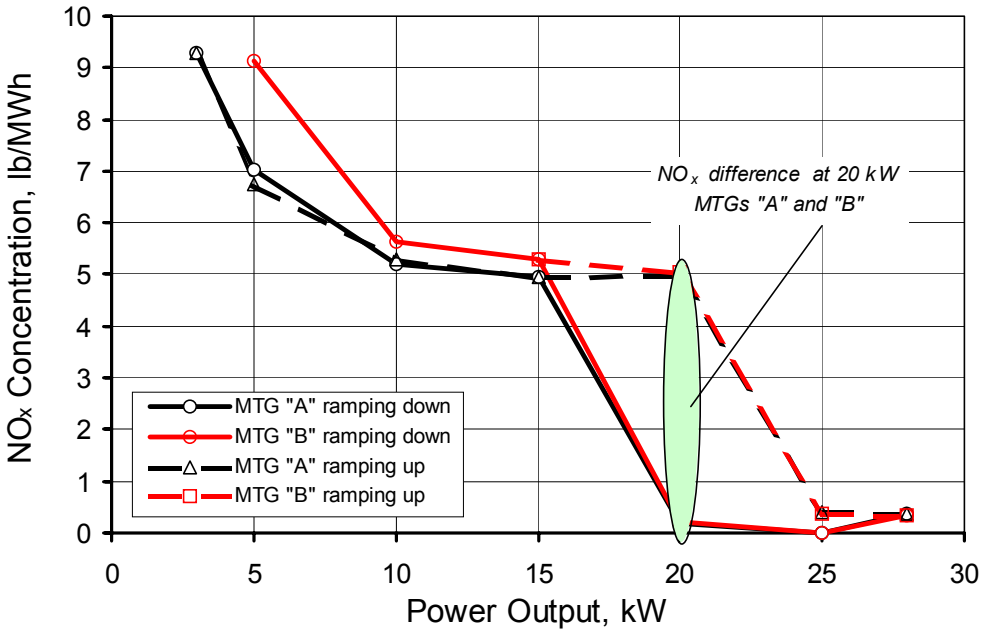

Figure 6. NO_x Concentration (lb/MWh) Versus the Power Output of MTGs A and B.

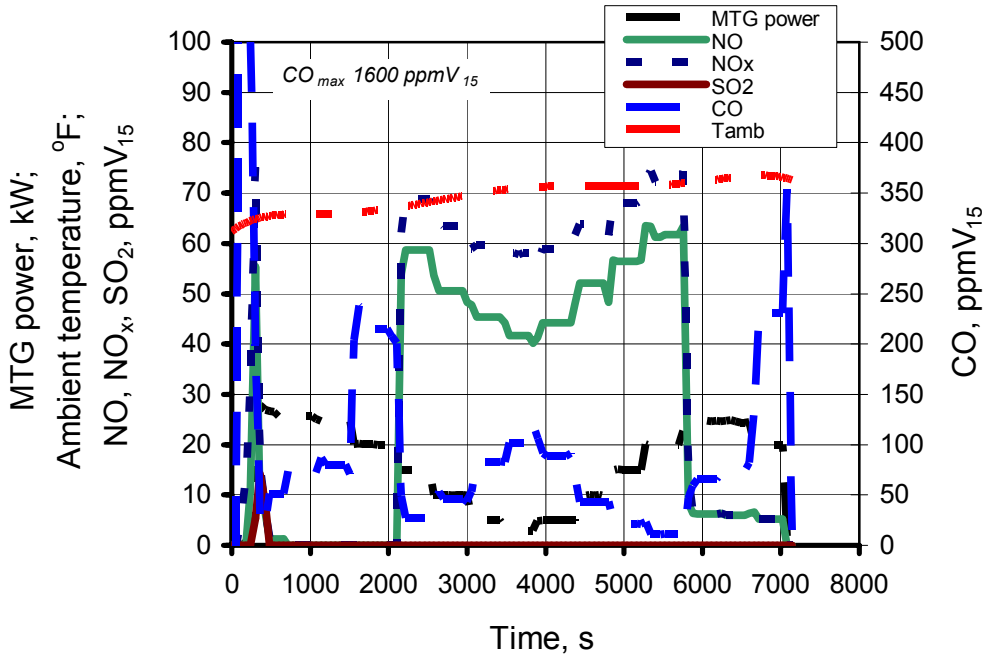

Figure 7. Concentration of Emission Impurities ($ppmV_{15}$) of MTG A During Startup, Shutdown, and Power Dispatch.

Emissions Study of a 70-kW MTG C

As it was mentioned above, the emission tests of MTG C were performed at one power output (~60 kW), which was governed by ambient conditions. Figure 8 shows the dynamic behavior of the emissions with time. It is evident that this machine produces the lowest emissions of all the MTGs considered in this study. Only during startup and shutdown do significant peaks of CO and NO_x appear (and no SO_2 at all), but during steady-state operation no CO was found in the flue gas, and the maximum amount of NO_x was 0.9 $ppmV_{15}$ (1.7 mg/m^3, or 0.05 lb/MWh). The latter "lb/MWh" value refers to the electrical portion of the total power generated; however, if we consider the thermal energy produced in the built-in HRU, the NO_x emissions reduce to 0.02 lb/MWh. All these measured values are much less than emission limits given by the manufacturer (9 $ppmV_{15}$ or 0.25 lb/MWh CO and 9 $ppmV_{15}$ or 0.41 lb/MWh NO_x). Considering other emissions standards, these data would comply with even the most stringent CARB regulations to be in effect in 2007.

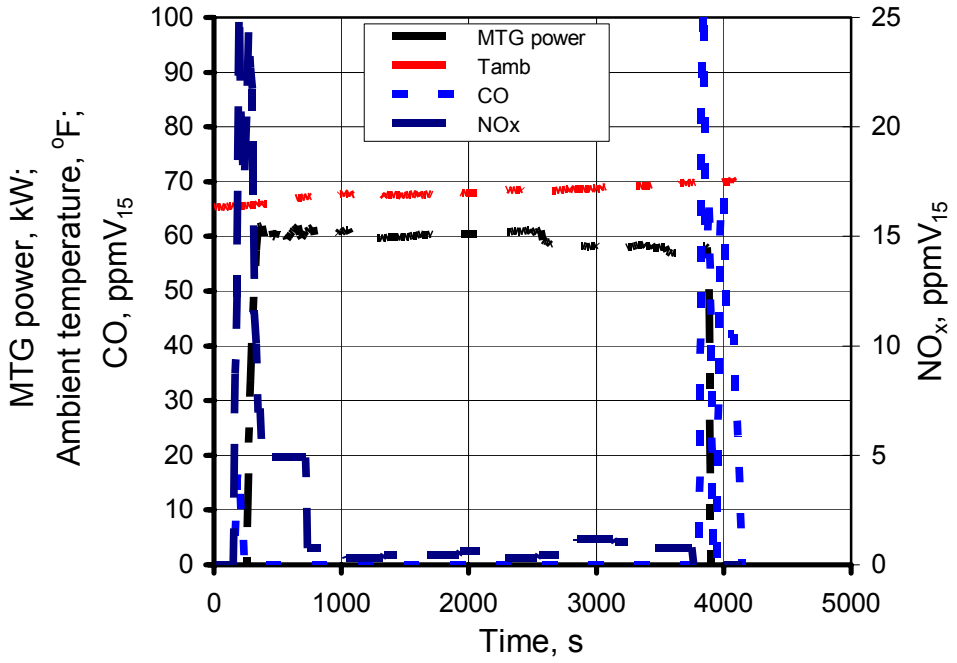

Figure 8. CO and NO_x Concentrations ($ppmV_{15}$) for the MTG C During Startup, Shutdown, and Power Dispatch.

Effect of Power Output on Emissions Rate of 80-kW MTG D

The emission tests on MTG D were performed over the power output range of 1/16 (5 kW) to almost full power output (75 kW). Due to operational limits of the MTG, it was not possible to study the emissions performance at the maximum 80 kW output. Figures 9-11 present the dependencies of CO and NO_x emissions on power output in ppmV at 15% O_2 ($ppmV_{15}$), mg/m^3 and lb/MWh. Results obtained from MTG D are different from the previous case with the two 30-kW MTGs (A and B): at the maximum power output studied (75 kW), the CO emissions reached its minimum at 51 $ppmV_{15}$ (58 mg/m^3 or 1.9 lb/MWh) CO, but the NO_x emissions reached its maximum at 27 $ppmV_{15}$ (52 mg/m^3 or 1.7 lb/MWh). These data are higher than the limits specified by the MTG manufacturer (30 $ppmV_{15}$ CO and 25 $ppmV_{15}$ NO_x), although it should be emphasized that these limits are for the MTG's maximum power output of 80 kW. The NO_x concentration in the MTG flue gas at 75 kW is significantly lower than the data reported for the 100 kW reciprocating engine. However, NO_x concentration in the MTG D is approximately 3.4 (1.7/0.5) times higher than the 2003 CARB emissions standards.

A decrease in the MTG D power output significantly increases the CO emissions and reduces the NO_x emissions to zero.

The dynamic change of the MTG D emissions with time and power output is shown in Figure 12. There is a very high CO peak during startup. NO_x at all studied power outputs consisted only of NO. No SO_2 was found in emission samples both during startup and steady-state operation of this MTG.

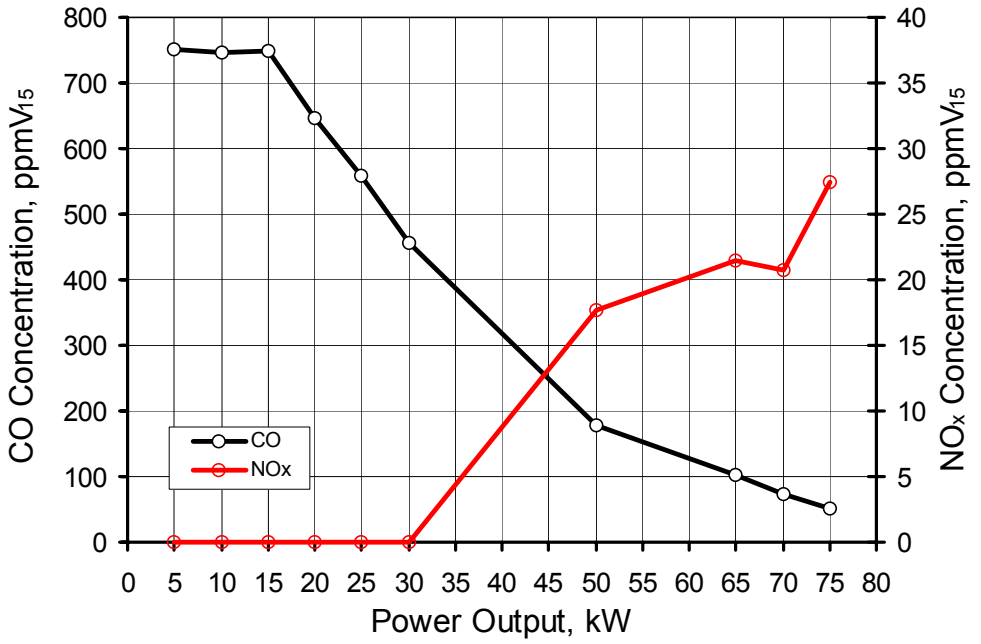

Figure 9. CO and NO_x Concentrations ($ppmV_{15}$) Versus the Power Output of MTG D.

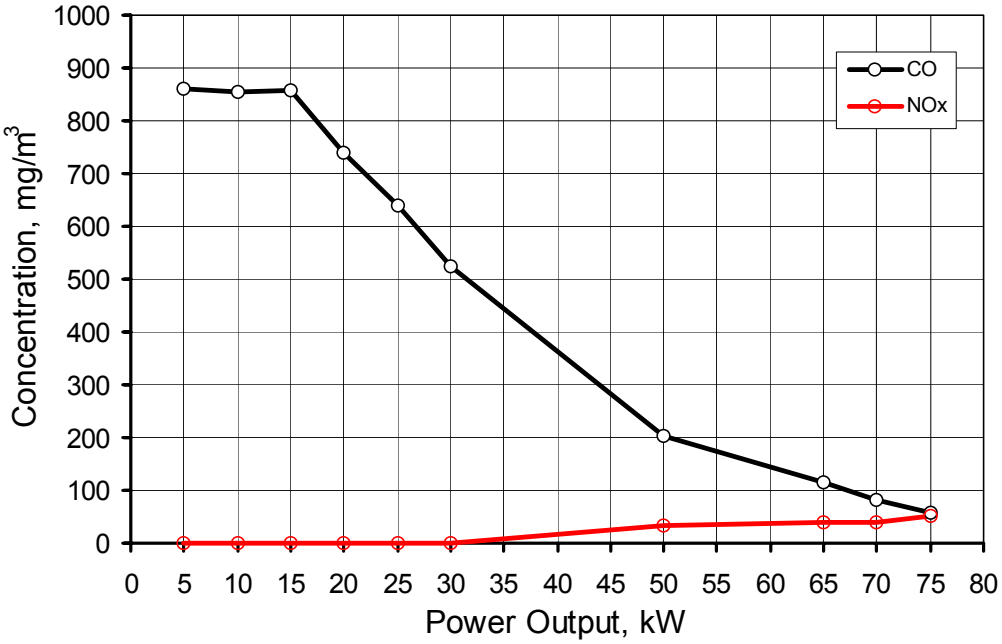

Figure 10. CO and NO_x Concentrations (mg/m^3) Versus the Power Output of MTG D.

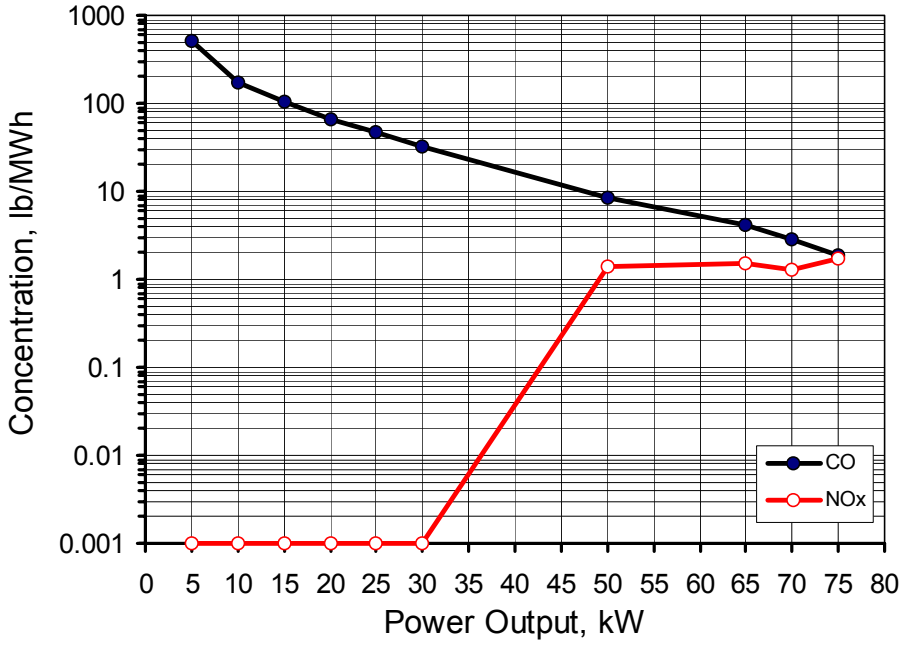

Figure 11. CO and NO_x Concentrations (lb/MWh) Versus the Power Output of MTG D.

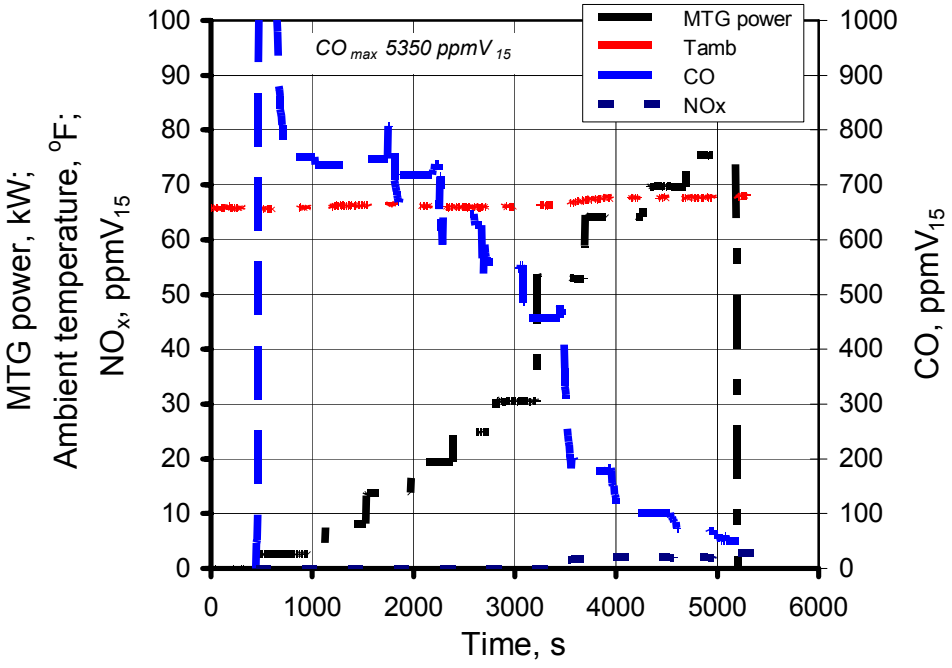

Figure 12. CO and NO_x Concentrations ($ppmV_{15}$) of MTG D During Startup, Shutdown, and Power Dispatch.

Comparison of Emissions Performance of the Different MTGs Involved in This Study

The comparison of emissions performance of the different MTGs within this study shows that at maximum power output the minimum levels of NO_x and CO in exhaust gas are produced by the 70-kW MTG C, and the maximum by the 80-kW MTG D (Figures 13-15). The latter MTG also operates at the highest excess air (>1000%) as compared with other MTGs studied with relatively large oxygen content in the exhaust gas (Figure 16). Higher oxygen values in the exhaust gas inevitably result in the higher oxygen-corrected ppmV (and, subsequently, mg/m^3 and lb/MWh) values, provided measured ppmV values are the same. The only emissions component of the MTG D operation that is lower as compared with the operation of the other MTGs is CO_2, but again it is related to higher oxygen content in the MTG exhaust gas (Figure 17).

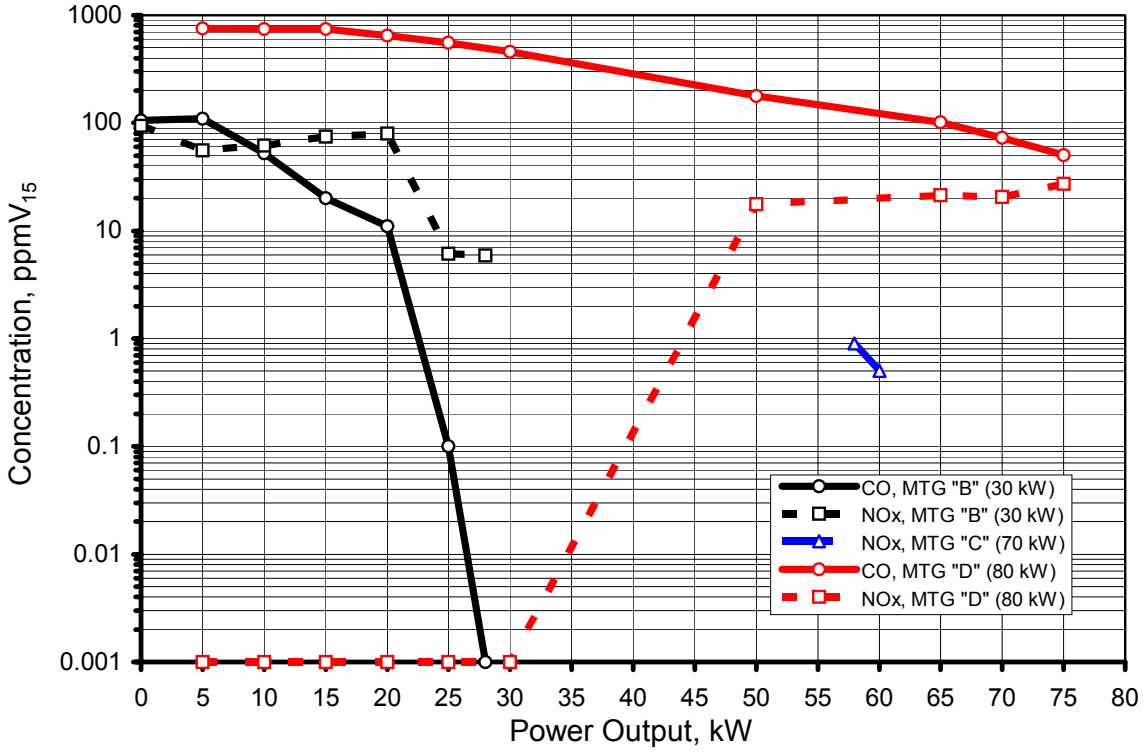

Figure 13. CO and NO_x Concentrations ($ppmV_{15}$) Versus the Power Output of Different MTGs.

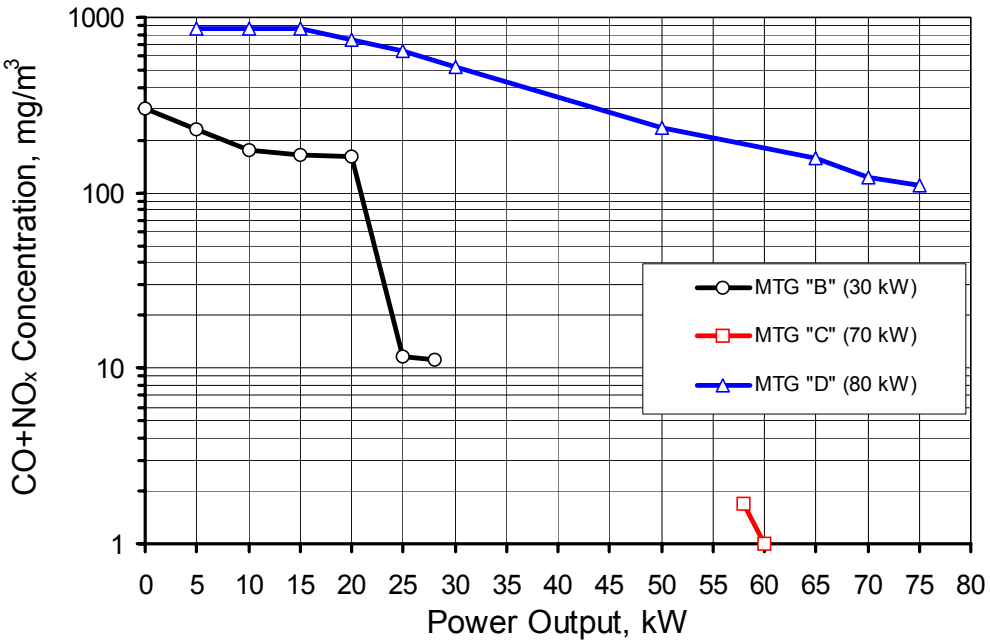

Figure 14. $CO+NO_x$ Concentration (mg/m^3) Versus the Power Output of Different MTGs.

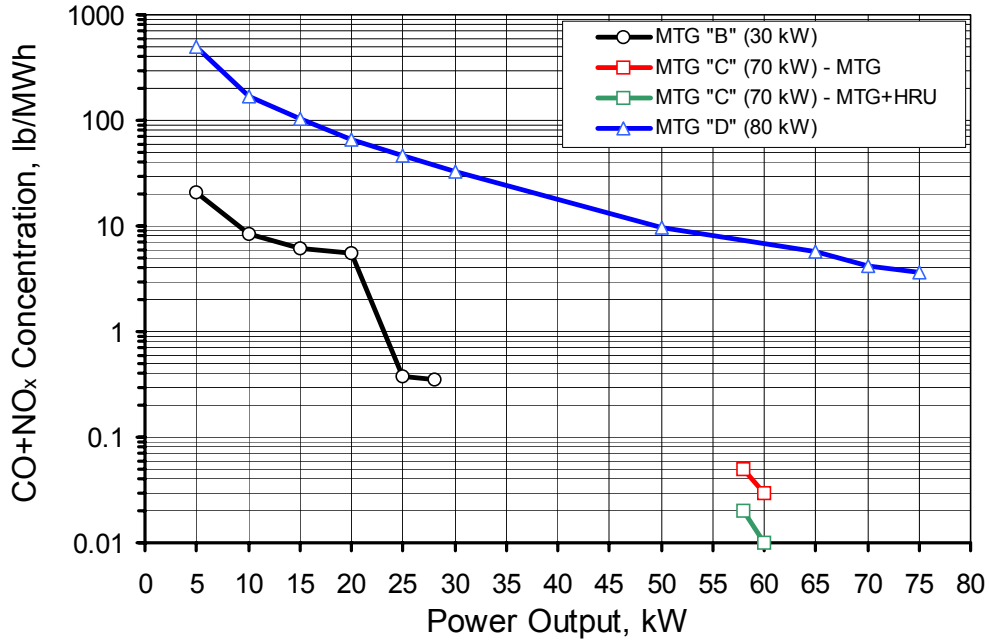

Figure 15. $CO+NO_x$ Concentration (lb/MWh) Versus the Power Output of Different MTGs.

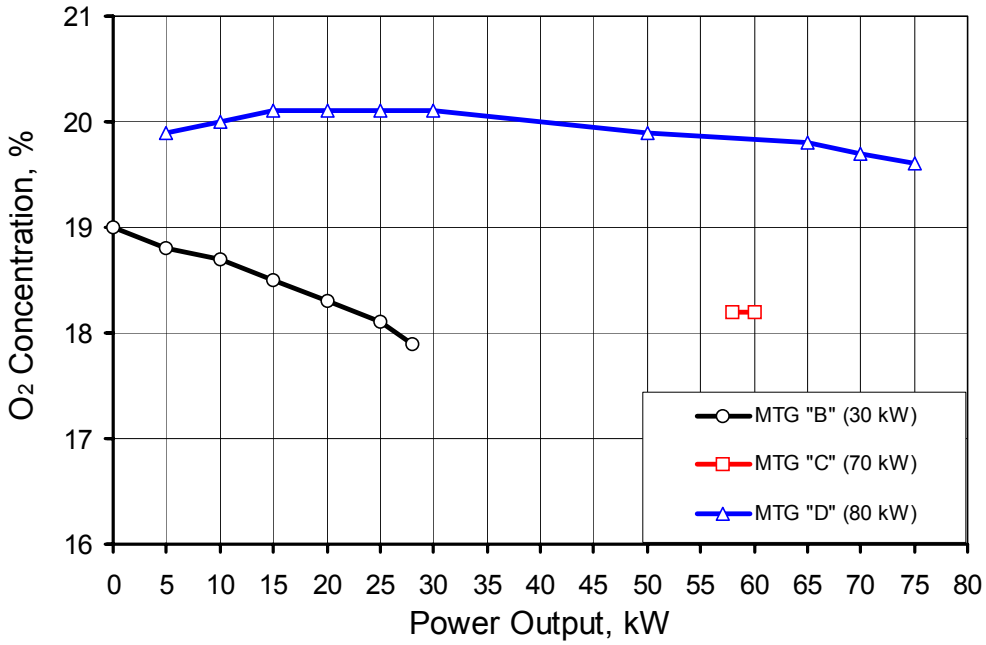

Figure 16. O_2 Concentration Versus the Power Output of Different MTGs.

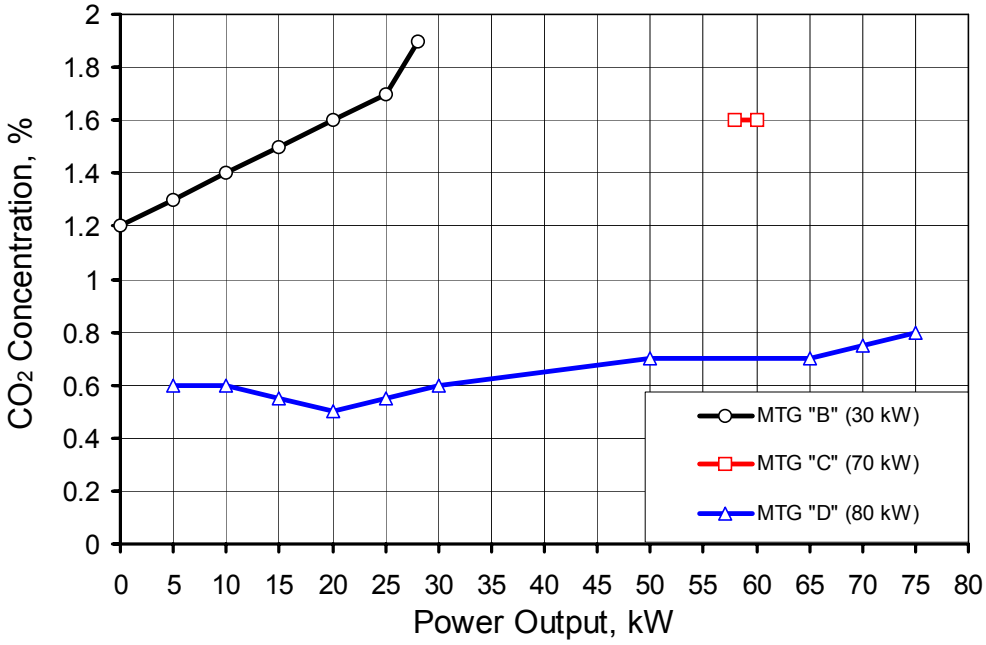

Figure 17. CO_2 Concentration Versus the Power Output of Different MTGs.

CONCLUSIONS

In summary, the emissions tests (at ORNL and EPRI PEAC) of four MTGs of different makes and sizes at different power output have been conducted to determine the level of emissions at both steady-state and transient operations. For steady-state tests, emissions were measured at different MTG power output levels for 15 to 20 minute periods. For transient tests, emissions levels were measured as the MTG power output was varied during startup, shutdown, and power dispatch (increase or decrease of power output).

At full power output, the 30-kW MTGs (A and B) were found to produce 0-19 $ppmV_{15}$ (0-22 mg/m^3 or 0-0.7 lb/MWh) CO and *ca.* 6 $ppmV_{15}$ (11 mg/m^3 or 0.4 lb/MWh) NO_x. The measured NO_x emissions at full power output were found to be less than the manufacturer's specified value and are within the 2003 CARB limits for DG equipment. The 70-kW MTG C at the maximum studied power output (60 kW) produced only 0.9 $ppmV_{15}$ (1.7 mg/m^3, or 0.05 lb/MWh) NO_x and no CO during steady-state operation. This is less than values specified by the manufacturer and is within the CARB limits that will be introduced in 2007. The emissions rates of the 80-kW MTG D at the maximum studied power output (75 kW) were 51 $ppmV_{15}$ (58 mg/m^3 or 1.9 lb/MWh) CO and 27 $ppmV_{15}$ (52 mg/m^3 or 1.7 lb/MWh) NO_x. These values are higher than the limits specified by the manufacturer, and the NO_x level in the exhaust gas exceeds the 2003 CARB limits.

Overall the results of the MTG emission tests for various power output levels are as follows:

- The lowest emission levels were measured with the 70-kW MTG C, and the highest levels with the 80-kW MTG D. The MTG C is the only MTG of those studied with emission levels that are within the proposed 2007 CARB limits.
- No SO_2 emissions were encountered in this study for any of the MTGs; therefore, there is no potential for the dewpoint corrosion of the low-temperature path of IES systems using these MTGs.
- Operation of the MTGs at reduced power output levels increases the cumulative emissions ($CO+NO_x$) of flue gas components which can result in exceeding existing emissions limits specified by manufacturers and government institutions.
- Significantly greater levels of CO concentration can be reached during MTG startup (MTGs A, B, and D) and shutdown (MTG C).
- As a rule, oxygen content and excess air increase as the MTG power output is reduced, while the CO_2 concentration decreases. Both excess air and the CO_2 concentration were not measured directly, but were calculated using fuel input data and the oxygen concentration in the MTG's flue gas. The maximum O_2 and minimum CO_2 levels in the flue gas were found with the 80-kW MTG D.
- Testing results suggest that there may be opportunity to lower part load emissions with revised engine control schemes and methods.

ACKNOWLEDGEMENTS

The authors would like to thank the Office of Energy Efficiency and Renewable Energy, U.S. DOE, for supporting this work. This research was also supported in part by an appointment to ORNL Postdoctoral Research Associates Program administered jointly by the Oak Ridge Institute for Science and Education and ORNL. This work was conducted by ORNL under DOE contract DE-AC05-00OR22725 with UT-Battelle, LLC. The work by PEAC was sponsored by DOE and EPRI Members of Completing the Circuit (Duke Energy, Lincoln Electric Service,

Texas Utilities, Alliant Energy, Cinergy, Southern Company, and Public Service of New Mexico). The work by PEAC was conducted under ORNL purchase order 4000008315.

REFERENCES

1. Popovic P., Marantan A., Radermacher R., and Garland P., "Integration of Microturbine with Single-Effect Exhaust-Driven Absorption Chiller and Solid Wheel Desiccant System." ASHRAE Transactions, 2002, vol. 108, pp. 1-9, paper HI-02-5-3.
2. Fairchild P.D., Labinov S.D., Zaltash A., and Rizy D.T., "Experimental and Theoretical Study of Microturbine-Based BCHP System." Proceedings of the 2001 International ASME Congress and Exposition, IMECE 2001 / AES-23622, November 11-16, 2001, New York, NY, USA, pp. 1-12. Available at the 2001 Congress CD.
3. Strategic Plan For Distributed Energy Resources, Office of Energy Efficiency and Renewable Energy and Office of Fossil Energy, U.S. Department of Energy, Washington, D.C., 2000. Available from http://www.eren.doe.gov/der/documents_resources.html.
4. Labinov S.D., Zaltash A., Rizy D.T., Fairchild P.D., DeVault R.C., and Vineyard E.A., "Predictive Algorithms for Microturbine Performance for BCHP Systems." ASHRAE Transactions, 2002, vol. 108, pp. 1-12, paper HI-02-5-4.
5. More Stringent Environmental Standards Favor Microturbines. IR Energy Systems, Davidson, NC, USA. Available from http://www.irpowerworks.com.
6. California DG Program. Paper presented at 2003 CHP Turbine Technology and Turbine Regulatory Forum, San Diego, CA. Available from http://www.arb.ca.gov/energy/dg/dg.htm.
7. Petrov A.Yu., Zaltash A., Rizy D.T., and Labinov S.D. Environmental Aspects of Operation of a Gas-Fired Microturbine-Bades CHP System. Proceedings of the 19th Annual International Pittsburgh Conference "Coal – Energy and Environment". September 23-27, 2002, Pittsburgh, PA. Available at the 2002 Annual Conference CD.
8. 1997 National Air Quality: Status and Trends. Published by the Office of Air & Solutions, U.S. Environmental Protection Agency. The document is available from http://www.epa.gov/oar/aqtrnd97/brochure.
9. Gabrielli F., Goodstine S., and Mastronarde T, "Cold-End Corrosion in HRSGs". PowerPlant Chemistry, 2002, vol. 4, No. 3, pp. 148-153.
10. Brewster B.S., Cannon S.M., Farmer J.R., and Meng F., "Modeling of Lean Premixed Combustion in Stationary Gas Turbines." Progress in Energy and Combustion Science, 1999, vol. 25, pp. 353-385.
11. Sarkisov A.A., Rudakov O.A., Salivon N.D., Sigalov Yu.V., and Mitrofanov V.A., "The Generalized Emissions Characteristic of a Gas-Turbine Engine as a Function of the Design and Operating Parameters of the Combustion Chamber." Thermal Engineering, 2000, vol. 47, No. 4, pp. 352-355.
12. ENERAC Integrated Emissions System, Model 3000E. Instructions Manual. Energy Efficiency Systems, Westbury, NY, USA, 1998. Available from http://www.enerac.com/.
13. Code of Federal Regulations, Title 40: Protection of Environment; Chapter 1: Environmental Protection Agency; Part 60: Standards of Performance for New Stationary Resources; Paragraph 335: Test Methods and Procedures, 1999. Available from http://www.access.gpo.gov/nara/cfr/waisidx_99/40cfr60_99.html.
14. Beychok M.R. Fundamentals Of Stack Gas Dispersion. Newport Beach, CA, USA, 1995.
15. Hammerschlag R. Method 19 Calculator. Institute for Lifecycle Energy Analysis, Seattle, WA, USA. Available from http://www.ilea.org/downloads/Method19.xls.

16. Foley G. and Sweetser R., “Emerging Role for Absorption Chillers in Integrated Energy Systems in America.” Paper presented at the International Mechanical Engineering Congress and Exposition Emerging and New Technologies for Heat Pump and Refrigeration Cycles and CHP (Combined Cooling, Heating and Power), November 17-22, 2002, New Orleans, LA, USA.